RSC Advances

This is an *Accepted Manuscript*, which has been through the Royal Society of Chemistry peer review process and has been accepted for publication.

Accepted Manuscripts are published online shortly after acceptance, before technical editing, formatting and proof reading. Using this free service, authors can make their results available to the community, in citable form, before we publish the edited article. This *Accepted Manuscript* will be replaced by the edited, formatted and paginated article as soon as this is available.

You can find more information about *Accepted Manuscripts* in the Information for Authors.

Please note that technical editing may introduce minor changes to the text and/or graphics, which may alter content. The journal's standard Terms & Conditions and the Ethical guidelines still apply. In no event shall the Royal Society of Chemistry be held responsible for any errors or omissions in this *Accepted Manuscript* or any consequences arising from the use of any information it contains.

ROYAL SOCIETY OF CHEMISTRY

www.rsc.org/advances

Journal Name

ARTICLE

Enhanced Performance of TiO_2 Ultraviolet Detector Modified with Graphene Oxide

Received 00th January 20xx,
Accepted 00th January 20xx

DOI: 10.1039/x0xx00000x

www.rsc.org/

Dezhong Zhang,[a] Fuyi Jing,[b] Fengli Gao,[b] Liang Shen,[b] Dongming Sun,[a] Jingran Zhou,*[a] Yu Chen,*[c] and Shengping Ruan*[b]

The performance of Schottky metal-semiconductor-metal (MSM) ultraviolet (UV) photodetector is limited by the insufficient gain and the uncontrollable noise current. A remarkable detectivity UV detector is demonstrated based on graphene oxide (GO) modified TiO_2 with high gain and low noise. The GO layer completely prevents the flow of electrons forming hole-only device thus decreasing the dark current and noise current, furthermore, gain of the holes is promoted under UV illumination. Moreover, the GO layer efficiently extracts the holes therefore reducing the fall time. Under a bias of 6 V, the responsivity value reaches 826.8 A/W and the noise current is only 1.8 pA, thereby, our device provides a detectivity of 2.82×10^{13} cm $Hz^{1/2}$ W^{-1} at 280 nm. The results offer an effective approach to enhance the performance of UV detector.

1. Introduction

Sensing of ultraviolet (UV) light is critical for a variety of industrial and scientific applications, including light-wave communications, remote control, environmental monitoring, imaging techniques, as well as in future memory storage and optoelectronic circuits.[1-6] Nowadays, wide band-gap semiconductor UV photodetectors have attracted significant attention for their immediate application to replace the conventional devices based on expensive single-crystalline silicon or polycrystalline silicon.[7-9] Various wide band-gap semiconductors have been investigated for UV photodetectors due to their intrinsic visible-blindness, especially oxide semiconductors such as TiO_2, ZnO, and SnO_2, which are environmental friendly as well as thermally and chemically stable.[10-12] Amongst the different materials studied thus far, TiO_2, an n-type wide band-gap semiconductor (anatase 3.2 eV and rutile 3.0 eV), is widely researched and used, obtaining a series of devices with significant detectivity, such as the Bi doped TiO_2 device of 4.741×10^8 cm $Hz^{1/2}$ W^{-1},[13] the TiO_2 nanoparticles and silicon nanowires hybrid device of 2.44×10^{10} cm $Hz^{1/2}$ W^{-1},[14] and TiO_2 nanotube device of 1.5×10^{12} cm $Hz^{1/2}$ W^{-1}.[15] Meanwhile, TiO_2 is also employed to the device with Schottky metal-semiconductor-metal (MSM) structure.[16-18] The MSM devices have a multitude of positive properties such as the high working repeatability and the fast response speed,[19-21] however, the lack of gain and the difficulty of limiting the noise current have still restricted its commercial application. How to solve these problems are the crucial issues to achieve an excellent performance of the MSM devices employing inorganic wide band-gap semiconductor materials and make it possess stronger temptation in the UV detector field.

Graphene oxide (GO), a polymer-like graphitic semiconductor made of only carbon, oxygen, and hydrogen, has been employed to photocatalys and solar cells due to its large exposed area, high stability and carrier mobility.[22, 23] In this work, the GO material, possessing the peculiar energy level structure and well electrical conductivity,[24-26] is employed to modify the Schottky contact between TiO_2 and Au electrodes, leading to the improved performance of MSM structure devices. In the absence of illumination, GO layers will block the electron transport, not only from TiO_2 layer to anode but also from cathode to TiO_2 layer, which limits the increase of the dark current, thus reducing the noise current of devices. Under UV illumination, GO layers could play different roles, when connecting to the anode (called AGO), it could reduce the hole potential barrier, while, it could effectively extract holes from TiO_2 layer when closing to the cathode (called CGO). At this point, only holes could be transported in the device, named single carrier device or hole-only device. Single carrier device can generate gain in its working process, which contributes to the enhancement of the responsivity and quantum efficiency. Hole-only device is excellent candidate to make a breakthrough on gain, noise and detectivity in the field of UV detection.

2. Experimental Section

All chemicals were purchased from Aladdin industrial corporation (Shanghai, China) and were used without further purification. The TiO_2 film was prepared on the quartz substrate by the sol-gel method.[27] The thickness of the TiO_2 film was about 100 nm. Then the windows in the shape of cross fingers on TiO_2 film were fabricated by the lithography method. Thereafter, GO was

[a] State Key Laboratory on Integrated Optoelectronics, Jilin University, Changchun 130012, P. R. China.
[b] College of Electronic Science and Engineering, Jilin University, Changchun 130012, P. R. China.
[c] Institute of Semiconductors, Chinese Academy of Sciences, Beijing 100083, P. R. China.

This journal is © The Royal Society of Chemistry 20xx

RSC Advances Accepted Manuscript

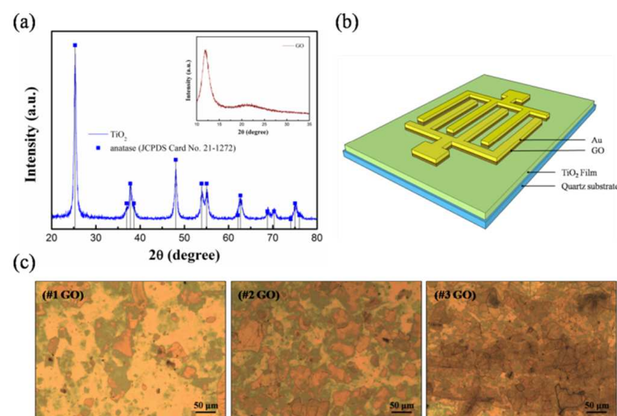

Fig. 1 (a) XRD pattern of TiO_2 material and insert is XRD pattern of GO material. (b) The structure diagram of GO modified TiO_2 UV detector. (c) Micro graphs of the GO distribution with 6000, 4000 and 2000 rpm.

synthesized from natural graphite powder using the Hummer's method. The GO layer was prepared by vacuum filtration of the GO aqueous solution through a membrane filter (0.22 μm in pore size), which was spin-coated at the speed of 6000 rpm for 20 s to remove the overmuch GO solution, followed by air drying at room temperature. Meanwhile the speeds of 4000 rpm and 2000 rpm have also been employed to obtain GO layer. In addition, the GO layer was fabricated into the same interdigital shape as the electrodes by using lithographic techniques. Subsequently, the Au interdigitated electrodes were fabricated by the magnetron sputtering technique. Both of the finger width and the spacing were 20 μm and the total active area was 0.38 mm^2.

The crystal structure of the films was examined by X-ray diffraction (XRD) on a Shimadzu XRD-6000 diffractometer. The absorption spectra were measured on a Shimadzu UV-1700 Pharma Spec UV spectrophotometer. The current-voltage (*I-V*) characteristics and responsivity of the devices were measured using a Keithley 2601 source meter together with a UV power meter. The time response characteristics were obtained by an oscilloscope. The noise current was measured by the Advantest R9211C FFT servo analyzer.

3. Results and discussion

Fig. 1a illustrates the XRD pattern of the as prepared pure TiO_2 material. The curve shows that all the reflection peaks of pure TiO_2 can be indexed to the anatase TiO_2 phase (JCPDS Card No. 21-1272), and no impurity peaks are observed, indicating that the final product is pure phase TiO_2 compound. The inset of Fig. 1a shows the XRD analysis of prepared GO exhibiting a layered nanostructure, as evidenced by the diffraction peak at $2\theta = 11.8^{\circ}$, which corresponds to a d-spacing of 0.75 nm. Fig. 1b shows the structure diagram of the device. When testing the photoelectric performance, the device is illuminated by UV light from the side of quartz substrate. Due to the symmetry of the device structure, the direction of the applied bias has no effect on the operation of the device. In the diagram, the GO material can be only found between the Au interdigital electrodes and the TiO_2 film, which avoid TiO_2 layer being short-circuited by

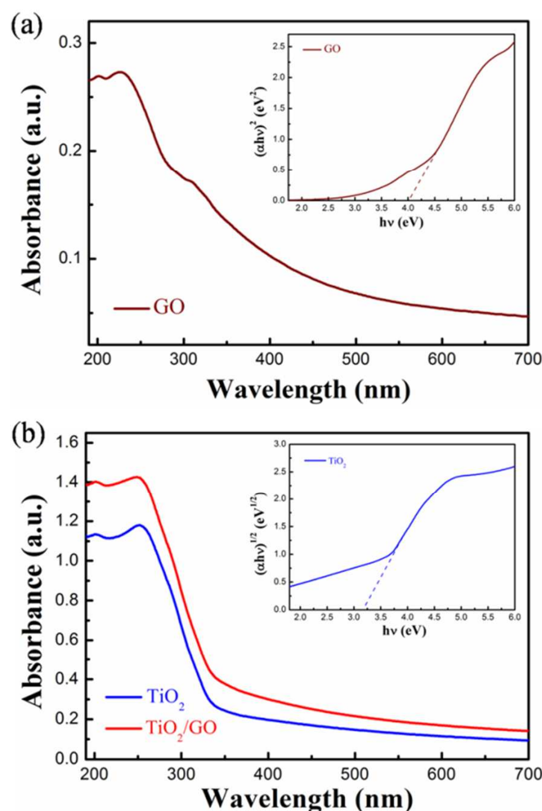

Fig. 2 UV-visible absorption spectra of (a) GO layer and (b) pure TiO_2 film and TiO_2/GO hybrid film. Insert of (a) presents variation of $(ahv)^2$ vs hv to obtain the direct optical absorption band-gap of GO. Insert of (b) shows variation of $(ahv)^{1/2}$ vs excitation energy (hv) to identify the band-gap of TiO_2.

the GO layer, meanwhile, the leakage current can be reduced effectively. Fig. 1c is the micro graphs of GO layers spin-coated by 6000, 4000 and 2000 rpm. The fabricated GO films with 6000, 4000 and 2000 rpm are named as #1 GO, #2 GO and #3 GO, respectively. The areas in dark of these three graphs are covered by GO sheet material. When the speed of spin-coating is fast (6000 rpm, the first graph), the GO sheets can not cover the substrate completely and the distribution is not uniform. If the speed drops to 4000 or 2000 rpm, the film can be formed basically and some areas may even overlap, meanwhile the color of films will become darker gradually.

To accurately evaluate the band-gaps of GO and TiO_2, the UV-Vis absorption spectra are measured and shown in Fig. 2. The absorption spectrum for GO in Fig. 2a with an absorption onset at ca. 500 nm shows two absorption edges at around 250 nm and 400 nm, which demonstrates that the as-prepared GO has the nature of an indirect band-gap semiconductor. Theoretical band structure analysis for graphene shows that the gap nature of graphene changes from direct to indirect with increasing oxidation level.[28] Seen from the absorption of TiO_2 in Fig. 2b, the remarkable rising of the absorption intensity occurs within the wavelength range from 260 nm to 330 nm and the absorption peak is observed at 260 nm, which exhibits the significant UV sensitivity and solar blind property of the TiO_2 film.

RSC Advances Accepted Manuscript

 This journal is © The Royal Society of Chemistry 20xx

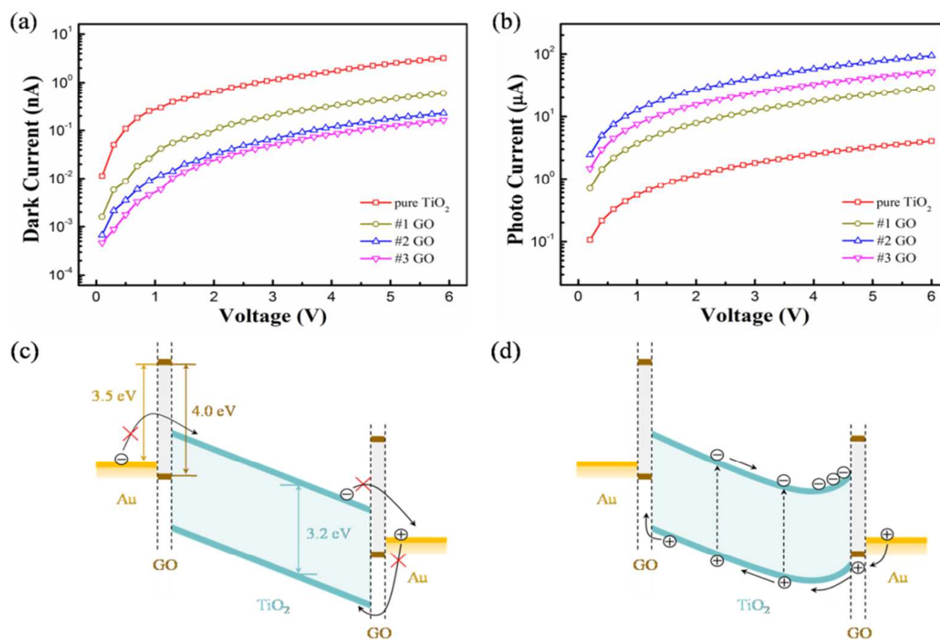

Fig. 3 The *I-V* characteristics of UV detectors (a) in dark and (b) under UV illumination. The corresponding energy level diagrams of GO device working (c) in dark and (d) with illumination.

The absorption spectrum of TiO_2/GO film was also measured. Compared with TiO_2 film, the GO (#2 GO) modified TiO_2 hybrid film possesses increased absorption intensity in the range of 190 nm to 700 nm, especially in the UV region. For most of the wide band-gap semiconductors, the optical absorption near the band edge has the following behavior:

$$\alpha = A\frac{(h\nu - E_g)^{n/2}}{h\nu} \quad (1)$$

where α is the optical absorption, A is a constant, h is Planck's constant, ν is the frequency, E_g is the semiconductor band-gap and n denotes the transition mode, which depends on whether the transition is direct (n = 1) or indirect (n = 4). Because GO exhibits strong direct optical absorption at ca. 250 nm, we take the value of 1 for the n in the Eq. (1) and plotted the square of $\alpha h\nu$ against $h\nu$. The insert of Fig. 2a gives apparent band-gap energy of 4.0 (± 0.05) eV for the GO specimen. The TiO_2, a type of indirect transition semiconductor, shows one sharp absorption edge for precise gap energy. We take the value of 4 for the n and 1 for the A in the Eq. (1), and plot the square root of the absorption energy ($\alpha h\nu$) against the photon energy ($h\nu$) to determine the band-gap of TiO_2. From approximate linear extrapolation, it can be obtained from the insert of Fig. 2b that the E_g of the TiO_2 film is 3.2 (± 0.06) eV.

To investigate the impact of GO films on the electrical properties, the *I-V* characteristics of the UV detectors in dark and under UV illumination are demonstrated in Fig. 3a and Fig. 3b, as well as corresponding energy level diagrams (the electron affinity of TiO_2 and GO are 4.3 and 1.6 eV)[29] are displayed in Fig. 3c and Fig. 3d, respectively. In dark, we can find that all devices with GO exhibit much lower dark currents compared with that of the pure TiO_2 device. Along with the increase of GO distribution, the dark current continues to decline. At 6 V bias, the dark current of the pure TiO_2 device is 3.20 (± 0.05) nA, more than 5 times higher than that of the #1 GO device (0.59 (± 0.03) nA). The dark currents of #2 GO and #3 GO device do not show continuous significant changes, which are 0.23 (± 0.02) nA and 0.16 (± 0.03) nA. We infer that the dark current can not perpetually reduce while tending to a saturation value with further increase of the GO distribution. Fig. 3b shows the *I-V* characteristics of the devices measured under UV illumination at the wavelength of 280 nm with 30.0 μW/cm^2 irradiation intensity. At the bias of 6 V, the #2 GO device has the highest photocurrent of 94.3 (± 0.1) μA, which is higher than the #1 GO device (28.7 (± 0.1) μA) and the pure TiO_2 device (4.04 (± 0.05) μA). Compared with #2 GO device, the photocurrent of the #3 GO device has not been promoted, but a modest decline. The analysis of the devices working mechanism can be depicted associating with the energy level diagrams. Fig. 3c shows that the CGO layer can block the external electron injection and AGO layer can prevent the electrons from transporting to anode. So, the dark current of GO devices mainly attributes to the hole current. However, the dark current of the pure TiO_2 device mainly arises from the electron current,[30] thus the former will be significantly reduced. With the increase of the GO distribution, the capacity of anode to block electron can be enhanced, therefore the dark current, theoretically concluding hole current only, will be further decreased and eventually tend to a steady state. Fig. 3d shows the energy level diagram under UV irradiation, the photo-generated carriers produce in the TiO_2. At this time, due to the strong extraction effect from CGO,[31, 32] the photo-generated holes will be

RSC Advances Accepted Manuscript

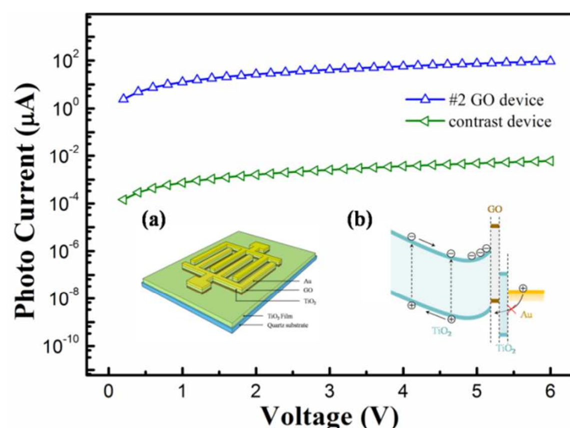

Fig. 4 The comparison of *I-V* characteristics of the #2 GO device and the contrast device under UV illumination. Insert of (a) presents the structure diagram and (b) shows the energy level diagram of the contrast device.

swept out of TiO_2 and flow to the cathode. Meanwhile, AGO will prevent the photo-generated electrons from being collected by the anode. Thus the photo-generated electrons will be accumulated in the vicinity of TiO_2 connected with AGO under the bias, leading to an increase of the electron barrier and a decrease of the hole barrier, the energy level of TiO_2 near the anode becomes bent. Therefore, holes have a greater probability to inject into the devices, which generates the gain of holes. In addition, we realize that photocurrents present the trend of firstly increase and then decrease with the increase of GO distribution. It could be explained that the increase of the AGO distribution is advantageous to improve the capacity to prevent electron transport, leading to a larger current by gain of holes. However, when the distribution of GO exceeds a certain range, the capacity of blocking electron will reach the limit and hole barrier will be formed easily by the excessively thick GO layer, which lead to the decrease of the photocurrent.

To further prove the GO modified TiO_2 UV detector is a hole-only device, we made some other comparative experiments that a TiO_2 layer is added between the Au electrodes and the GO layer. The new TiO_2 layer prepared by magnetron sputtering method can conduct electrons and block the holes. Fig. 4 shows the comparison of *I-V* characteristics of the #2 GO device and the contrast device, which demonstrates that the photocurrent of the contrast device has a sharp decline due to the incorporation of the new TiO_2 layer. The insert (a) is the structure diagram and (b) is the energy level diagram of the contrast device. Seen from the insert (b), due to the high hole injection barrier between Au and TiO_2, the holes will be effectively blocked by the new added TiO_2 layer. At this time, the holes can not inject into the device to form the gain of holes, leading to an apparent decrease of the photocurrent, and the device almost has no photo response. Therefore, we have verified that the GO modified TiO_2 UV detector is a hole only device.

A comparison of spectral response from 250 nm to 400 nm under 6 V bias is shown in Fig. 4a. It can be found that all the devices demonstrate response peaks at similar wavelengths (270 nm to 280 nm) of the UV light. The highest responsivity is supplied by the #2 GO device, which can reach 826.8 A/W at the wavelength of 280 nm. In addition, we convert the value of responsivity (R) into quantum efficiency (QE) by

$$QE = R \times h\nu \qquad (2)$$

where the $h\nu$ is the energy of the incident photon in electronvolts. The QE is 366,100% for the #2 GO device at 280 nm, which is much higher than 100% due to the existence of large gain. As for the response spectra curve from 280 nm to 360 nm in Fig. 2a, the response of all devices become negative, which is affected by weakened light absorption of the TiO_2 film. From 370 nm to 400 nm, all the UV detectors have low response. This is because the working state of the devices is close to dark state, and the responsivity depends on the dark current. Moreover, it is worth noting that all the response curves present downward trend under the irradiation of shorter wavelength UV light from 280 nm to 250 nm. This can be attributed to the strong absorption of high energy photons near the surface region of the semiconductor. The photo-generated carriers near the surface have shorter lifetime than those in the bulk, thus they contribute less to the photoresponse.[33]

The time response characteristics of the devices upon switching the UV light on and off are shown in Fig. 4b. The rise time (from 10% to 90% of the peak value) is 655 ms for pure TiO_2 device, 810

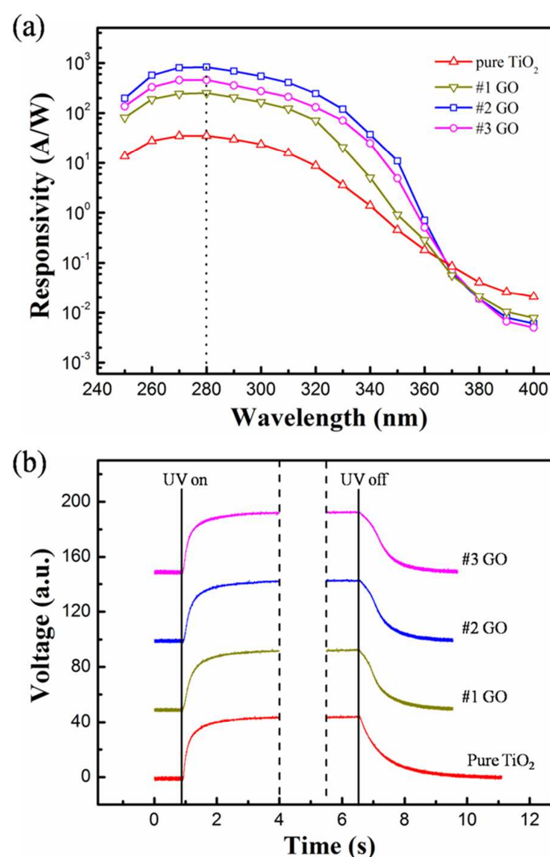

Fig. 5 (a) The spectral response and (b) time response characteristics of pure TiO_2 and GO modified TiO_2 UV detectors.

RSC Advances Accepted Manuscript

This journal is © The Royal Society of Chemistry 20xx

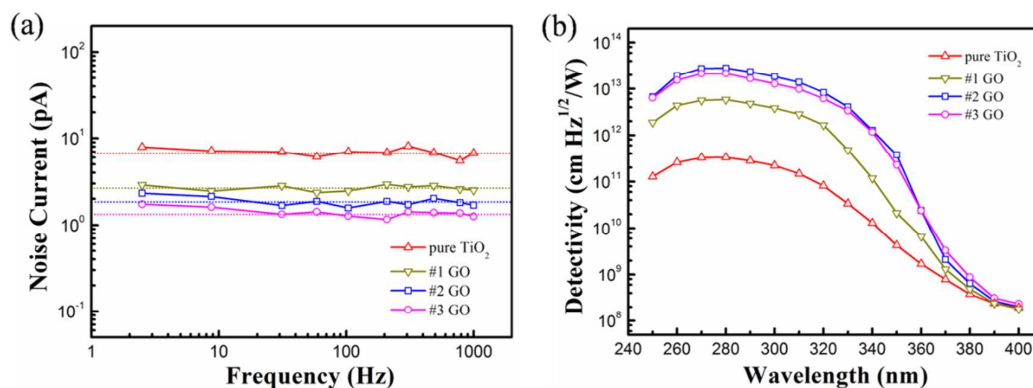

Fig. 6 (a) The noise currents of devices with frequency range from 1 Hz to 1 kHz. (b) Special detectivities of UV detectors at different wavelengths.

ms for #1 GO device, 834 ms for #2 GO device and 887 ms for #3 GO device. The rise time of devices with GO is slightly longer than that of the pure TiO_2 device. This is due to the photo-generated electron accumulation near the interface between TiO_2 and GO, which takes a period of time to reduce the hole barrier and achieve balance, therefore the rise time of the devices with GO is increased. In addition, we can find that with the enhanced distribution of the GO, the rise time displays a modest increase, which arises from the widened depletion region and lengthy drift distance, leading to a longer time before achieving balance, therefore, all of these confirm the above discussion about the accumulation of the photoinduced carrier. When switching off the UV light, the fall time (from 90% to 10% of the peak value) is 3.37 s for pure TiO_2 device, 1.74 s for #1 GO device, 1.80 s for #2 GO device and 1.89 s for #3 GO device. Compared with pure TiO_2 device, the obvious reduction in the fall time of GO devices is ascendant in the time response characteristics We can find that there are some differences for the tendency of the fall time between GO devices and pure TiO_2 device. For the GO devices, the fall time do not present the directly and fleetly decline trend, while firstly experiences a slow fall moment, which is due to the recombination of excess carriers and the recovery of hole barrier height after the illumination is withdrew, and then drops fast until under the 20 % of the peak value, the reason for this is the holes are heavily extracted by CGO, which makes a mainly contribution to the reduction of the fall time. Meanwhile, seen from these three GO devices, we can also find that the first period of fall time will be lengthened with the increased GO distribution, which associates with the characteristics of rise time.

In addition, the factor that limits the detectivity of UV detector is the noise, furthermore, the shot noise from the dark current is the major contribution to the total noise. To include other possible noise, such as flicker noise and thermal noise, the total noise current (I_n) of the devices was measured by an FFT servo analyzer with frequency range from 1 Hz to 1 kHz. As shown in Fig. 5a, the total noise current characteristics are found to be dominated by the shot noise and the noise current is reduced due to the incorporation of GO layer, which is consistent with the tendency of the dark current. The specific detectivities (D^*) of UV detector is given by the following[6]

$$D^* = \frac{(A\Delta f)^{1/2} R}{I_n} \tag{3}$$

where A is the effective area of the detector in cm^2, Δf is the frequency interval over which the noise is measured, R is the responsivity we obtained in the previous. The D^* of our devices are calculated at different wavelengths with the measured noise current and responsivity at 6 V bias. The comparison of spectral D^* from 250 nm to 400 nm is shown in Fig. 5b. The #2 GO device has the highest D^* from 250 nm to 360 nm, and the peak value reaches 2.82×10^{13} cm $Hz^{1/2}$ W^{-1} at 280 nm. For comparison, the D^* of our device is higher than some other TiO_2 devices, such as the TiO_2 nanoparticles and silicon nanowires hybrid device of 2.44×10^{10} cm $Hz^{1/2}$ W^{-1},[14] and TiO_2 nanotube device of 1.5×10^{12} cm $Hz^{1/2}$ W^{-1}.[15] Moreover, the D^* is also higher than that of some detectors based on other materials, such as the MoS_2 device of 5×10^7 cm $Hz^{1/2}$ W^{-1},[34] and NiO/ZnO heterojunction device of 1.6×10^{12} cm $Hz^{1/2}$ W^{-1}.[35]

4. Conclusions

In summary, we have investigated the effects of GO material on the performance of TiO_2 UV detector based on MSM structure. The optoelectronic properties, including *I-V* characteristics, time response and specific detectivity have been studied. Due to the blocking of electrons by GO layers, the hole-only device provides a lower dark current leading to the decrease of noise current, and a higher gain of holes leading to the increase of responsivity. Thus the specific detectivity is significantly increased, corresponding to an enhancement of 2 orders of magnitude for the #2 GO device compared with pure TiO_2 device. Owing to the extraction of holes by the GO layer, the fall time of GO device has been shortened. This application of GO material possesses a great potential for the research of UV detector.

Acknowledgments

This work was supported by the National Natural Science Foundation of China (Grant No. 61274068, 61404058, 61204055); Opened Fund of the State Key Laboratory on Integrated Optoelectronics (No. IOSKL2013KF10); Project of Science and Technology Plan of Changchun City (Grant No. 14KG020); Jilin Province Economic Structure Strategic Adjustment Special Plan (2014Y086).

RSC Advances Accepted Manuscript

This journal is © The Royal Society of Chemistry 20xx

Notes and References

1 N. Nasiri, R. H. Bo, F. Wang, L. Fu, A. Tricoli, *Adv. Mater.* 2015,**27**, 4336-4343.
2 Z. H. Lin, G. Cheng, Y. Yang, Y. S. Zhou, S. Lee, Z. L. Wang, *Funct. Mater*. 2014, **24**, 2810-2816.
3 L. Peng, L. F. Hu, X. S. Fang, *Adv. Mater.* 2013, **25**, 5321-5328.
4 E. Cicek, R. McClintock, A. Haddadi, W. Rojas, M. Razeghi, *IEEE J Quantum Elect.* 2014, **50**, 593-597.
5 T. Y. Zhai, X. S. Fang, M. Y. Liao, X. J. Xu, L. Li, B. D. Liu, Y. Koide, Y. Ma, J. N. Yao, Y. Bando, D. Golberg, *Acs Nano* 2010, **4**, 1596-1602.
6 X. Gong, M. H. Tong, Y. J. Xia, W. Z. Cai, J. S. Moon, Y. Cao, G. Yu, C.-L. Shieh, B. Nilsson, A. J. Heeger, *Science* 2009, **325**, 1665-1667.
7 R. J. Zou, Z. Y. Zhang, Q. Liu, J. Q. Hu, L. W. Sang, M. Y. Liao, W. J. Zhang, *Small* 2014, **10**, 1848-1856.
8 U. Schühle, J.-F. Hochedez, In *Observing Photons in Space*, Springer: 2013; pp 467-477.
9 L. Li, E. Auer, M. Y. Liao, X .S. Fang, T. Y. Zhai, U. K. Gautam, A. Lugstein, Y. Koide, Y. Bando, D. Golberg, *Nanoscale* 2011, **3**, 1120-1126.
10 Y. R. Xie, L. Wei, Q. H. Li, Y. X. Chen, S. S. Yan, J. Jiao, G. L. Liu, L. M. Mei, *Nanotechnology* 2014, **25**, 075202.
11 S. M. Peng, Y. K. Su, L. W. Ji, C. Z. Wu, W. B. Cheng, W. C. Chao, *J. Phys. Chem. C* 2010, **114**, 3204-3208.
12 H. Chen, L. F. Hu, X. S. Fang, L. M. Wu, *Adv. Funct. Mater*. 2012, **22**, 1229-1235.
13 S. N. Mazhir, G. H. Mohamed, A. A. Abdullah, M. D. Radhi, *Int. J. Adv. Res*. 2015, **3**, 1060-1070.
14 K. Rasool, M. A. Rafiq, M. Ahmad, Z. Imran, M. M. Hasan, *Appl. Phys. Lett.* 2012, **101**, 253104
15 M. Z. Wang, F. X. Liang, B. Nie, L. H. Zeng, L. X. Zheng, P. Lv, Y. Q. Yu, C. Xie, Y. Y. Li, L. B. Luo, *Part. Part. Syst. Char.* 2013, **30**, 630-636.
16 H. L. Huang, Y. N. Xie, W. F. Yang, F. Zhang, J. F. Cai, Z. Y. Wu, *IEEE Electr. Device L.* 2011, **32**, 530-532.
17 D. Çalışkan, B. Bütün, Ş. Özcan, E. Özbay, *Opt. express* 2014, **22**, 14096-14100.
18 X. H. Gu, F. X. Meng, G. H. Liu, H. F. Zhang, J. R. Zhou, S. P. Ruan, *Chem. Commun*. 2013, **49**, 6328-6330.
19 Y. N. He, W. Zhang, S. C. Zhang, X. Kang, W. B. Peng, Y. L. Xu, *Sensor Actuat. A: Phys.* 2012, **181**, 6-12.
20 J. Xing, H. Y. Wei, E.-J. Guo, F. Yang, *J. Phys. D Appl. Phys.* 2011, **44**, 375104.
21 D. Gedamu, I. Paulowicz, S. Kaps, O. Lupan, S. Wille, G. Haidarschin, Y. K. Mishra, R. Adelung, *Adv. Mater*. 2014, **26**, 1541-1550.
22 T. F. Yeh, J. M. Syu, C. Cheng, T. H. Chang, H. Teng, *Adv. Funct. Mater* 2010*,* **20***,* 2255-2262.
23 S.-S. Li, K.-H. Tu, C.-C. Lin, C.-W. Chen, M. Chhowalla, *ACS Nano* 2010, **4**, 3169-3174.
24 K. Krishnamoorthy, M. Veerapandian, K. Yun, S.-J. Kim, *Carbon* 2013, **53**, 38-49.
25 L. L. Zhang, X. Zhao, M. D. Stoller, Y. W. Zhu, H. X. Ji, S. Murali, Y. P. Wu, S. Perales, B. Clevenger, R. S. Ruoff, *Nano lett.* 2012, **12**, 1806-1812.
26 N. Yousefi, M. M. Gudarzi, Q. B. Zheng, S. H. Aboutalebi, F. Sharif, J.-K Kim, *J. Mater. Chem* 2012, **22**, 12709-12717.
27 M. Zhang, X. H. Gu, K. B. Lv, W. Dong, S. P. Ruan, Y. Chen, H. F. Zhang, *Appl. Surf. Sci*. 2013, **268**, 312-316.
28 J. Ito, J. Nakamura, A. Natori, *J. Appl. Phys.* 2008, **103**, 113712.
29 H.-L. Yip, A. K.-Y. Jen, *Energ. Environ. Sci.* 2012, **5**, 5994-6011.
30 A. Balducci, M. Marinelli, E. Milani, M. E. Morgada, A. Tucciarone, G. Verona-Rinati, M. Angelone, M. Pillon, *Appl. Phys. Lett.* 2005, **86**, 193509.
31 B. R. Lee, J.-w. Kim, D. Kang, D. W. Lee, S.-J. Ko, H. J. Lee, C.-L. Lee, J. Y. Kim, H. S. Shin, M. H. Song, *Acs Nano* 2012, **6**, 2984-2991.
32 D. Yang, L. Y. Zhou, L. C. Chen, B. Zhao, J. Zhang, C. Li, *Chem. Commun*. 2012, **48**, 8078-8080.
33 Y. L. Cao, Z. T. Liu, L. M. Chen, Y. B. Tang, L. B. Luo, J. S. Jie, W. J. Zhang, S. T. Lee, C. S. Lee, *Opt. Express* 2011, **19**, 6100-6108.
34 W. Choi, M. Y. Cho, A. Konar, J. H. Lee, G.-B. Cha, S. C. Hong, S. Kim, J. Kim, D. Jena, J. Joo, *Adv. Mater*. 2012, **24**, 5832-5836.
35 N. Park, K. Sun, Z. L. Sun, Y. Jing, D. L Wang, *J. Mater. Chem. C* 2013, **1**, 7333-7338.

RSC Advances Accepted Manuscript

This journal is © The Royal Society of Chemistry 20xx